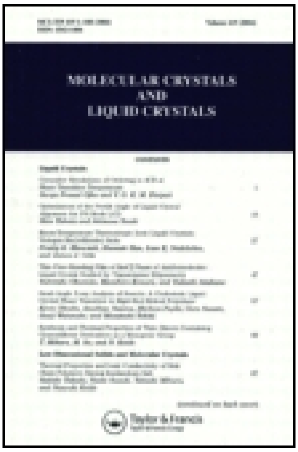

Molecular Crystals and Liquid Crystals
Publication details, including instructions for authors and subscription information:
http://www.tandfonline.com/loi/gmcl20

# Dielectric Spectroscopy of an Antiferroelectric Liquid Crystal for Two Cell Thicknesses

Suman Kumari [a], R. Dhar [b], I. M. L. Das [a] & R. Dabrowski [c]

[a] Department of Physics, University of Allahabad, Allahabad, India

[b] Department of Material Sciences, University of Allahabad, Allahabad, India

[c] Institute of Chemistry, Military University of Technology, Warsaw, Poland

Version of record first published: 30 Jun 2011

To cite this article: Suman Kumari, R. Dhar, I. M. L. Das & R. Dabrowski (2011): Dielectric Spectroscopy of an Antiferroelectric Liquid Crystal for Two Cell Thicknesses, Molecular Crystals and Liquid Crystals, 541:1, 87/[325]-95/[333]

To link to this article: http://dx.doi.org/10.1080/15421406.2011.570157

*Mol. Cryst. Liq. Cryst.*, Vol. 541: pp. 87/[325]–95/[333], 2011
Copyright © Taylor & Francis Group, LLC
ISSN: 1542-1406 print/1563-5287 online
DOI: 10.1080/15421406.2011.570157

Taylor & Francis
Taylor & Francis Group

# Dielectric Spectroscopy of an Antiferroelectric Liquid Crystal for Two Cell Thicknesses

SUMAN KUMARI,[1] R. DHAR,[2] I. M. L. DAS,[1] AND R. DABROWSKI[3]

[1]Department of Physics, University of Allahabad, Allahabad, India
[2]Department of Material Sciences, University of Allahabad, Allahabad, India
[3]Institute of Chemistry, Military University of Technology, Warsaw, Poland

*The dielectric spectroscopy of an antiferroelectric liquid crystal (S)-4-(1-methylheptyloxycarbonyl)phenyl-4′-(6-pentanoyloxyhex-1-oxy)biphenyl-4-carboxylate for its homogeneous anchoring has been carried out for 10 μm and 4 μm cell thicknesses. This study suggests that the dielectric strength of Goldstone mode of the SmC* phase is significantly diminished from ∼195 to ∼69, whereas its relaxation frequency is increased from ∼2 kHz to ∼4 kHz from the higher to lower cell thickness. Alternatively, these parameters for the soft mode detected in the SmA* phase and for the two antiferroelectric relaxation modes detected in the $SmC_A^*$ phase do not show any appreciable change with the cell thickness.*

**Keywords** Antiferroelectric; dielectric strength; Goldstone mode; relaxation frequency; soft mode

## 1. Introduction

Antiferroelectric order has been known to exist in liquid crystals since more than a decade and is now an intensely studied field of research. The great application potential of antiferroelectric liquid crystals (AFLCs) [1] has especially been demonstrated in sophisticated flat panel display prototypes, which have not yet reached manufacturing, due to the severe intrinsic problem of folds in the smectic layers, which drastically limit the achievable contrast, and which seems impossible to circumvent. This problem has been removed to a large extent by using orthoconic antiferroelectric liquid crystals (OAFLCs) [2]. In general their optical properties make them unique not only among liquid crystals but among electro-optical materials also. The AFLC material (S)-4-(1-methylheptyloxycarbonyl)phenyl-4′-(6-pentanoyloxyhex-1-oxy)biphenyl-4-carboxylate (4H6Bi(S)) belongs to the class of highly tilted AFLCs synthesized by Dabrowski's group from Warsaw [3,4]. The molecular structure of the material is given in the Figure 1.

---

Address correspondence to I. M. L. Das, Department of Physics, University of Allahabad, Allahabad-211002, India. Tel.: +91-532-2460993; Fax: +91-532-2460993; E-mail: profimldas@yahoo.com; suman2301@gmail.com

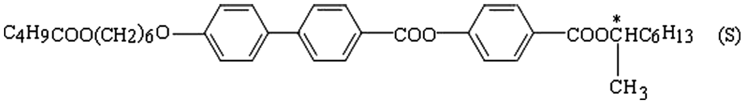

Figure 1. Molecular structure of the material 4H6Bi(S).

This material possesses high spontaneous polarization and microsecond response time which is advantageous for its application in displays. The temperature dependent dielectric spectroscopy and switching study of the material has been reported in our earlier publications [5,6]. In this paper the comparison of different relaxation parameters viz. dielectric strength ($\Delta\varepsilon_{\perp}$) and relaxation frequency ($f_R$) of various relaxation modes has been made for two different cell thicknesses.

## 2. Experimental

Dielectric spectra of the material have been recorded for its planar alignment in a parallel plate capacitor made form the ITO coated glass electrodes having sheet resistance 25 Ω/, in the frequency range 0.1 Hz – 10 MHz using impedance/gain-phase analyzer Solartron (model SI-1260) coupled with a Solartron dielectric interface (model 1296). The planar anchoring of the molecules was achieved by depositing a thin layer of polyamide nylon on electrodes and rubbing them unidirectional. Data acquisition process has been repeated for the two cell thicknesses: 10 μm and 4 μm during the cooling cycles with a probing electric field of 500 mVrms. A hot stage (Instec-HS-1) with an accuracy of ±0.1°C and the resolution limit of ±0.003°C has been used to control the sample temperature. The temperature near the sample has been determined by measuring thermo-emf of a copper-constantan thermocouple with the help of a six and half digit multimeter. The measured data have been analyzed by fitting of the dielectric spectra with the generalized Cole–Cole equation which is described in detail in reference [5]. The details of experimental technique and fitting model have been described elsewhere [5,7–11]. Although data have been acquired upto 10 MHz but above 1 MHz, high frequency parasitic effects are highly dominant and it could not be possible to extract correct data.

## 3. Results and Discussions

The dielectric data have been acquired during cooling cycle from the isotropic to the crystal phase. The compound is found to exhibit three distinguishing smectic phases viz. paraelectric SmA*, ferroelectric SmC* and antiferroelectric $\mathrm{SmC}_A^*$ phases by analysis of the data.

As already reported in our previous publication various relaxation modes have been detected during temperature dependent study of the material viz. soft mode (SM) in the SmA* and SmC* phases, Goldstone mode (GM) and a low frequency mode (LFM) in the SmC* phase and two relaxation modes separated by two decades of frequency in the $\mathrm{SmC}_A^*$ phase [5]. As an illustration the experimental, fitted and corrected data (after subtracting the low and high frequency artifacts from the experimental data) for dielectric permittivity ($\varepsilon'_{\perp}$) and loss ($\varepsilon''_{\perp}$) in the SmC* phase, have been plotted in the Figures 2(a) and 2(b) for the 10 and 4 μm cell thicknesses respectively. The low and high frequency artifacts are the increase of $\varepsilon'_{\perp}$ and $\varepsilon''_{\perp}$ at the low (below 100 Hz) and high (above 100 KHz) frequencies [8–11]. Which are reduced by using Cole-Cole equation [5,7].

The variation of $\varepsilon'_\perp$ with temperature for various frequencies has been shown in Figure 3. It is evident from the Figure 3 that $\varepsilon'_\perp$ possesses smaller value at all frequencies for the lower cell thickness. Temperature dependences of the $\Delta\varepsilon_\perp$ and $f_R$ of various relaxation modes for the two cell thicknesses have been demonstrated in Figures 4 and 5. The $\Delta\varepsilon_\perp$ and $f_R$ of SM are found to be almost independent of the cell thickness. The value of $\Delta\varepsilon_\perp$ of SM varies from 0.06 to 6.7 for 10 μm thick cell and from 0.06 to 8.5 for 4 μm thick cell in the temperature range 100.2 to 94.2°C [inset-1 of Figures 4(a) and (b)]. And its $f_R$ varies in the range 530–60 kHz for 10 μm and 420 – 47 kHz for 4 μm (Fig. 5).

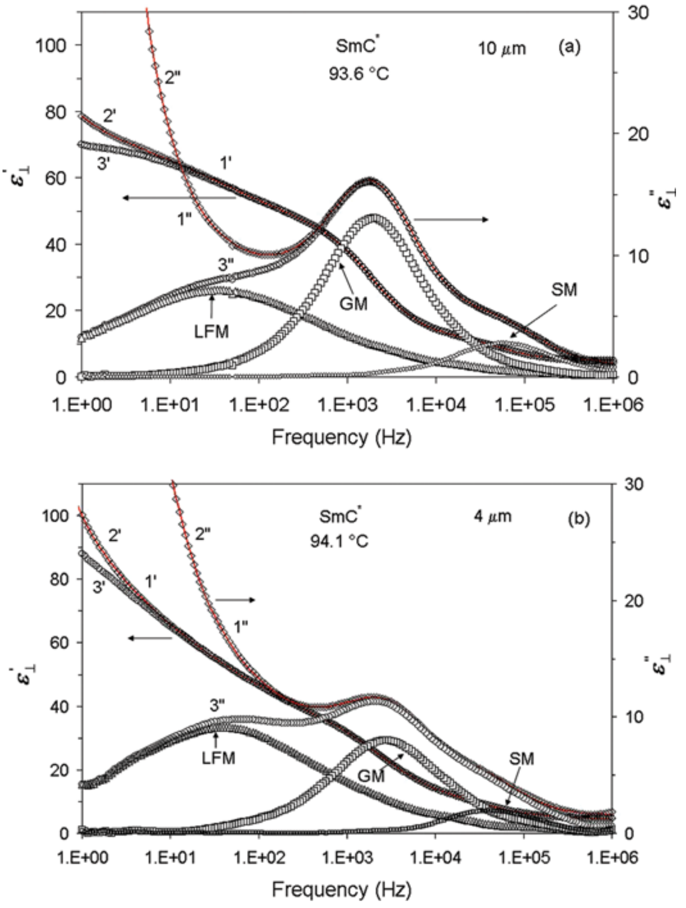

**Figure 2.** Frequency dependence of the dielectric permittivity ($\varepsilon'_\perp$) (primary axis) and dielectric loss ($\varepsilon''_\perp$) (secondary axis) for SmC* phase (a) at 93.6°C for 10 μm and (b) at 94.1°C for 4 μm. Curves 1, 2 and 3 (primed for ($\varepsilon'_\perp$) and double primed for ($\varepsilon''_\perp$)) represent the experimental, fitted and corrected data respectively. The LFM, GM and SM represent the $\varepsilon''_\perp$ data for these modes separately after removing the contribution of other modes and the low and high frequency artifacts. (Figure appears in color online.)

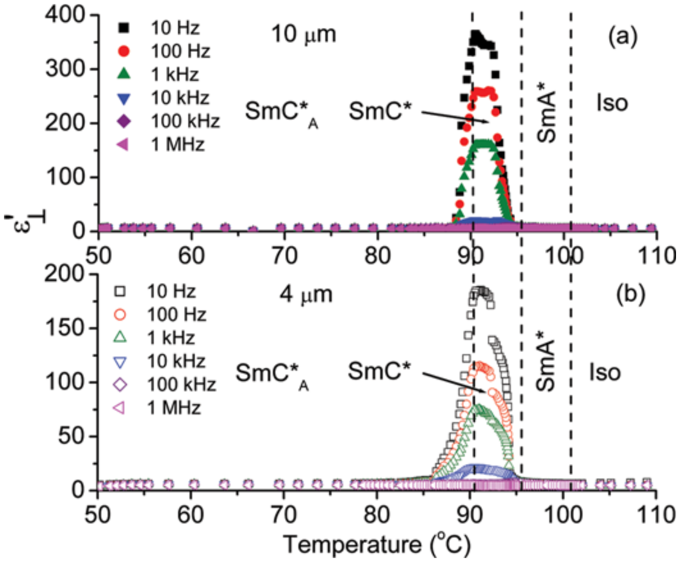

**Figure 3.** Temperature dependence of dielectric permittivity ($\varepsilon'_\perp$) in various phases of the material for (a) 10 μm and (b) 4 μm thicknesses. Vertical dashed lines indicate the separation of different phases on the basis of dielectric parameters. (Figure appears in color online.)

In the SmC* phase also, the $\Delta\varepsilon_\perp$ of SM is not much influenced by the variation of cell thickness. On the other hand, the dielectric parameters ($\Delta\varepsilon_\perp$ and $f_R$) of GM and LFM are largely affected by the cell thickness (Figs. 4 and 5). The plots of $\Delta\varepsilon_\perp$ and $f_R$ for GM only have been shown in the Figure 6 for the two cell thickness. $\Delta\varepsilon_\perp$ of GM is highly reduced. It is evident from the maximum value of $\Delta\varepsilon_\perp$ of GM, which is ~192 for 10 μm and ~69 for 4 μm. This is due to the surface interacting forces that hinder the phase angle fluctuation of directors in thin cell causing the helix of the SmC* phase to partially suppress. The relaxation frequency of GM is ~2 kHz for the 10 μm and ~4 kHz for the 4 μm cell thicknesses as shown in Figure 6. This result is in agreement with earlier work [12]. This is obviously due to surface interaction in the thin cell. In the lower thickness, the GM penetrates deeper into the $\mathrm{SmC}^*_A$ phase to a temperature lower than that of the higher thickness because of the struggle between the surface anchoring forces and the fluctuation in the microscopic spontaneous polarization direction.

LFM has been observed only in the SmC* phase and in the coexisting region of the $\mathrm{SmC}^*$–$\mathrm{SmC}^*_A$ phases for both the thicknesses. The disappearance of LFM in other phases is due to shifting of $\varepsilon''_\perp$ maxima of this mode towards the lower frequency side affected by the ionic effects. For the 10 μm thick cell, LFM has been observed around 35–45 Hz having very high $\Delta\varepsilon_\perp$ (maximum value ~195) which is comparable to that of GM (maximum value ~192) as depicted in Figure 4(a). While for 4 μm thick cell it is detected around 1–10 Hz with maximum $\Delta\varepsilon_\perp \sim 334$ ($\gg 69$; $\Delta\varepsilon_\perp$ of GM). Such behavior of the dielectric parameters of LFM is opposite to the behavior of the dielectric parameters of GM, i.e., $\Delta\varepsilon_\perp$ of LFM is significantly increased whereas $f_R$ is decreased for the lower thickness of the sample cell. T. Ray *et al.* attributed LFM due to the inhomogeneous distribution of ionic charges [12]. Moreover, if one assumes that LFM is ionic mode then it must be seen in the

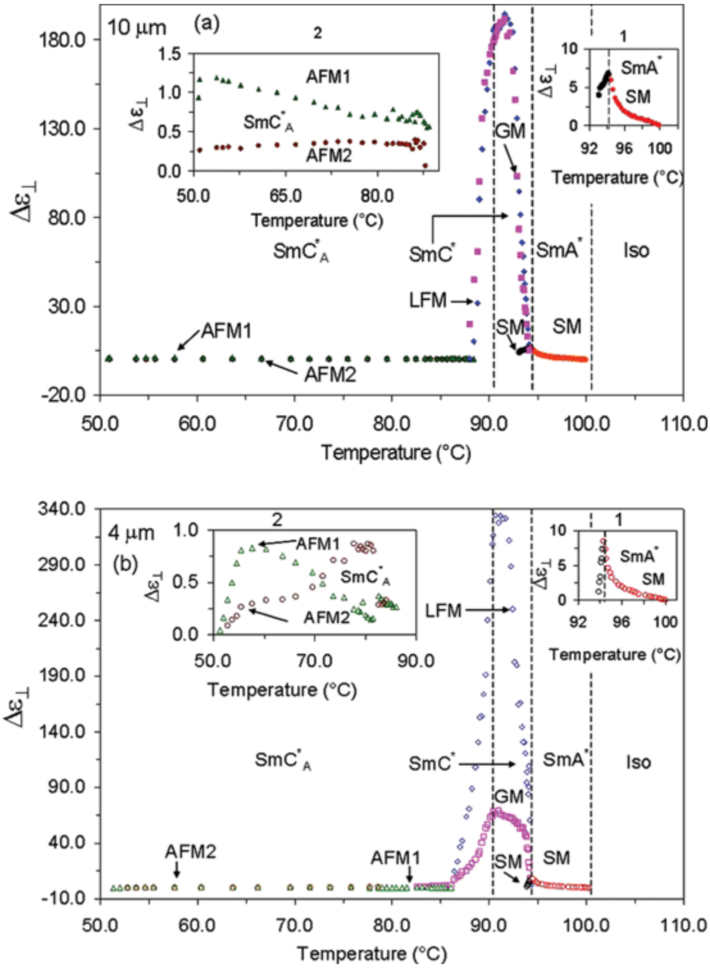

**Figure 4.** Temperature dependence of the dielectric strength ($\Delta\varepsilon_{\perp}$) in various phases of the material for (a) 10 μm and (b) 4 μm thicknesses. Insets-1 and 2 show expanded view of temperature dependence of the dielectric strength of the relaxation modes of SmA* and $\mathrm{SmC}_{\mathrm{A}}^{*}$ phases respectively.

SmA* phase also because SmA* phase shows high ionic conductance due to its occurrence at higher temperature as compared to the SmC* phase which is not the case. Hence, LFM can not be ionic mode. Beresnev *et al.* [13] have also reported two modes in the SmC* phase that were connected to the domain modes ($D_B$ and $D_S$ modes), but these modes could only be observed after suppression of Goldstone mode with bias electric field. As this mode appears even in the absence of the bias field, it may belong to an X-mode caused by distortion of azimuthal pretilt angle [14,15].

While going from the SmC* to the $\mathrm{SmC}_{\mathrm{A}}^{*}$ phase two relaxation modes (AFM1 and AFM2) appear at temperatures 88.4°C and 87.5°C respectively for 10 μm thick sample. However, these relaxation peaks have been observed rather at lower temperatures (at 86.0°C and 84.4°C) for the 4 μm thickness (Figs. 4 and 5). This is

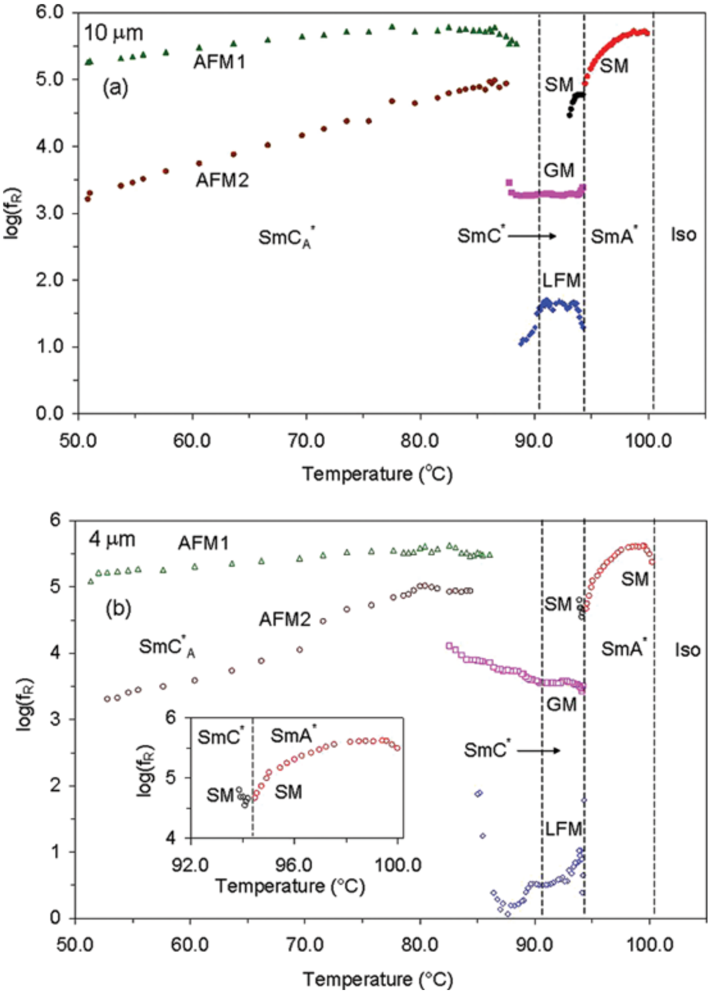

**Figure 5.** Temperature dependence of the relaxation frequency ($f_R$) in various phases of the material (a) 10 μm and (b) 4 μm thicknesses. Inset of (b) shows enlarge view of temperature dependence of relaxation frequency ($f_R$) of SM of SmA$^*$ and SmC$^*$ phases.

because of the effect of surface interaction on the mechanism of transformation of SmC$^*$ phase into the SmC$_A^*$ phase. As discussed earlier surface interacting forces hinder the disappearance of Goldstone mode due to coupling between these forces and the spontaneous polarization in the coexisting region of the SmC$^*$ and the SmC$_A^*$ phases. Hence, GM disappears at lower temperature that's why AFM1 and AFM2 appear at lower temperatures for the lower thickness. The variations of dielectric strengths of AFM1 and AFM2 for the two cell thicknesses have been shown in the inset-2 of Figures 4(a) and 4(b). These modes are separated by one to two decades of frequency as shown in the Figure 5. The relaxation frequencies of these modes are not significantly influenced by the cell thickness. These modes have also been found by several other workers for many AFLC compounds [16–20]. The mode AFM1 is due to the distortion of the antiferroelectric order

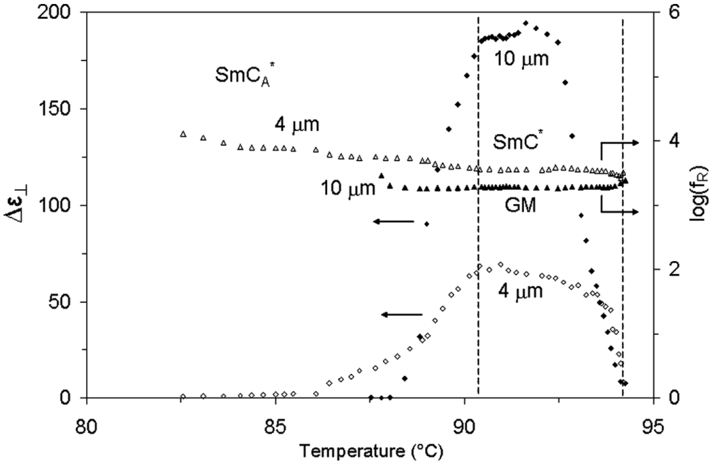

**Figure 6.** Comparison of dielectric strength ($\Delta\varepsilon_\perp$) (primary axis) and relaxation frequency ($f_R$) (secondary axis) of Goldstone mode for the 10 μm (filled symbols) and 4 μm (unfilled symbols) thicknesses.

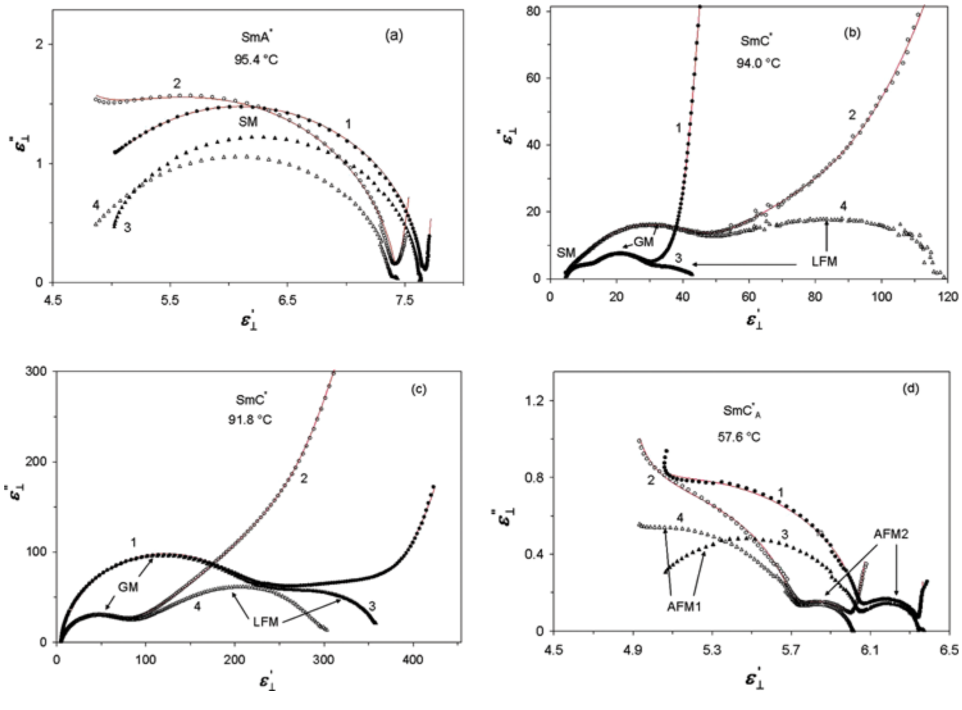

**Figure 7.** Cole–Cole plots of various relaxation modes of different phases. Filled symbols indicate data points for the 10 μm while unfilled symbols for the 4 μm thicknesses. 1, 2 represent the experimental data and 3, 4 the corrected data after removing the low and high frequency corrections. Red line over curves 1 and 2 represents the best fitted curve. (Figure appears in color online.)

caused by the antiphase motion and we call it the antiphase antiferroelectric Goldstone mode [16]. The mode AFM2 is assigned to the helix distortion mode as suggested by Panarin *et al.* [17].

The Cole-Cole plots (for both the thicknesses) have been plotted in the Figure 7 for all the modes existing in the various phases of the compound. The plot shows that the data points lie on a semicircle with centre below the $\varepsilon'_{\perp}$ axis implying $h > 0$. However, the data points deviate from the semicircle for extreme lower and higher frequency regime.

## 4. Conclusions

The study of the material 4H6Bi(S) for the two thicknesses suggests that the dielectric strength and relaxation frequency of soft mode is independent of the cell thickness where as that of the low frequency mode and the Goldstone mode are highly affected by the cell confinement. Due to the surface interacting forces acting on the phase fluctuation process occurring in the SmC* phase, the dielectric strength decreases but the relaxation frequency increases for the Goldstone mode with the decreasing cell thickness. The dielectric parameters of the low frequency mode are affected in a manner opposite to the Goldstone mode. The dielectric strength and relaxation frequency of the antiphase antiferroelectric Goldstone mode and the helix distortion mode are not affected by the cell thickness.

## Acknowledgment

We thank the Department of Science & Technology, Government of India for financial assistance under a research project (Grant no. SR/S2/CMP–45/2004). One of the authors (S.K.) also thanks CSIR (New Delhi) for providing SRF.

## References

[1] Chandani, A. D. L., Ouchi, Y., Takezoe, H., Fukuda, A., Terashima, K., Furukawa, K., & Kishi, A. (1989). *Jpn. J. Appl. Phys.*, *28*, L1261; Chandani, A. D. L., Gorecka, E., Ouchi, Y., Takezoe, H., & Fukuda, A. (1989). *Jpn. J. Appl. Phys.*, *28*, L1265.

[2] D'have, K., Rudquist, P., Lagerwall, S. T., Pauwels, H., Drzewiński, W., & Dabrowski, R. (2000). *Appl. Phys. Lett.*, *76*, 3528.

[3] Drzewiński, W., Dąbrowski, R., & Czupryński, K. (2002). *Polish J. Chem.*, *76*, 273.

[4] Gasowaska, J., Dabrowski, R., Drzewiński, W., Filipowicz, M., Przedmojski, J., & Kenig, K. (2004). *Ferroelectrics*, *309*, 83.

[5] Kumari, S., Dhar, R., Pandey, M. B., Das, I. M. L., & Dabrowski, R. (2009). *J. Phys. Chem. Sol.*, *70*, 316.

[6] Kumari, S., Pandey, M. B., Dhar, R., Das, I. M. L., & Dabrowski, R. (2011). *Phase Transitions*, *84*, 38.

[7] Hill, N. E., *et al.* (1969). *Dielectric Properties and Molecular Behaviour*, Van Nostrand Reinhold: London, pp. 48–54.

[8] Gouda, F. M. (1992). Dielectric relaxation spectroscopy of chiral smectic liquid crystal PhD. Thesis, Chalmer's University of Technology S-41296 Goteberg, Sweden, pp. 78–82 and 107–113; Gouda, F., Skarp, K., & Lagerwall, S. T. (1991). *Ferroelectrics*, *113*, 165.

[9] Srivastava, S. L., & Dhar, R. (1991). *Ind. J. Pure Appl. Phys.*, *29*, 745.

[10] Dhar, R. (2004). *Ind. J. Pure Appl. Phys.*, *42*, 56.

[11] Perkowski, P. (2010). *Phase Transitions*, *83*, 836.
[12] Ray, T., Kundu, S., Roy, S. K., & Dabrowski, R. (2007). *J. Mol. Liq.*, *113*, 104.
[13] Beresnev, L., Pfeiffer, M., Pikin, S., Haase, W., & Blinov, L. (1992). *Ferroelectrics*, *132*, 99.
[14] Panarin, Y. P., Xu, H., Lughadha, S. T., & Vij, J. K. (1994). *Jpn. J. Appl. Phys.*, *33*, 2648.
[15] Kundu, S. K., & Yagihara, S. (2007). *Jpn. J. Appl. Phys.*, *46*, 3211.
[16] Buivydas, M., Gouda, F., Lagerwall, S. T., & Stebler, B. (1995). *Liq. Cryst.*, *18*, 879.
[17] Panarin, Y. P., Kalinovskaya, O., & Vij, J. K. (1998). *Appl. Phys. Lett.*, *72*, 1667; Panarin, Y. P., Kalinovskaya, O., & Vij, J. K. (1998). *Liq. Cryst.*, *25*, 241.
[18] Hou, J., Schacht, J., Gie*β*elmann, F., & Zugenmaier, P. (1997). *Liq. Cryst.*, *22*, 409.
[19] Pandey, M. B., Dhar, R., & Dabrowski, R. (2008). *Phil. Magz.*, *88*, 101.
[20] Kumar, A., Dhar, R., Agrawal, V. K., Dabrowski, R., & Tykarska, M. (2008). *J. Appl. Phys.*, *104*, 054104.